THE IMMERSED INTERFACE METHOD FOR ELLIPTIC EQUATIONS WITH DISCONTINUOUS COEFFICIENTS AND SINGULAR SOURCES*

RANDALL J. LEVEQUE† AND ZHILIN LI‡

Abstract. The authors develop finite difference methods for elliptic equations of the form

$$\nabla \cdot (\beta(x)\nabla u(x)) + \kappa(x)u(x) = f(x)$$

in a region Ω in one or two space dimensions. It is assumed that Ω is a simple region (e.g., a rectangle) and that a uniform rectangular grid is used. The situation is studied in which there is an irregular surface Γ of codimension 1 contained in Ω across which β, κ, and f may be discontinuous, and along which the source f may have a delta function singularity. As a result, derivatives of the solution u may be discontinuous across Γ. The specification of a jump discontinuity in u itself across Γ is allowed. It is shown that it is possible to modify the standard centered difference approximation to maintain second order accuracy on the uniform grid even when Γ is not aligned with the grid. This approach is also compared with a discrete delta function approach to handling singular sources, as used in Peskin's immersed boundary method.

1. Introduction. Consider the elliptic equation

$$(1.1) \qquad\qquad \nabla \cdot (\beta \nabla u) + \kappa u = f$$

in a domain Ω in one, two, or three space dimensions. Within the region Ω, suppose there is an irregular surface of codimension 1 (hereafter called an interface) across which the function u or some of its derivatives are known to be discontinuous. For simplicity we assume that Ω is a simple domain, such as a square in two dimensions, and that we wish to solve the equation using a finite difference method on a regular grid, e.g., a uniform Cartesian grid. The interface is typically not aligned with the grid but rather cuts between grid points so that for grid points near the interface the stencil of a standard finite difference method will contain points from both sides of the interface. Because of the nonsmoothness of u, differencing u across the interface using standard difference formulas will not produce accurate approximations to derivatives of u, and hence a naive discretization will produce results with low accuracy.

For discontinuities to arise in the solution or its derivatives, there must be discontinuities or singularities present in the coefficients of the equation. Suppose, for example, that the function β is discontinuous across the interface, while κ and f are continuous. Then u and $\beta \partial u / \partial n$ will be continuous while the normal derivative $\partial u / \partial n$ will be discontinuous. Such problems arise frequently, for example, at the interface between two materials with different diffusion parameters in steady state heat diffusion or electrostatic problems. A Poisson problem with discontinuous coefficients also arises in multicomponent flow problems, e.g., the porous media equations used

---

† Departments of Mathematics and Applied Mathematics, University of Washington, Seattle, Washington 98195 (rjl@amath.washington.edu).

‡ Department of Applied Mathematics, University of Washington, Seattle, Washington 98195 (zhilin@amath.washington.edu).

to model the interface between oil and an injected fluid in simulations of secondary recovery in oil reservoirs [2], [5], [25].

Tikhonov and Samarskii [26] discuss the one-dimensional problem and the derivation of second-order methods on uniform grids using the jump conditions at a point of discontinuity in the coefficients. In two dimensions, Mayo [20] has considered similar problems and has shown how standard difference formulas can be modified to obtain second-order accuracy in the context of solving Poisson or biharmonic equations on irregular regions. The region is embedded in a regular region where a fast solver can be used on a uniform grid and the right-hand side is appropriately modified near the original boundary. Mayo and Greenbaum [22] consider an interface problem in magnetostatics of the form (1.1) with a piecewise constant coefficient β. The possibility of extension to variable β is mentioned in [21].

MacKinnon and Carey [18] also use a similar approach in one dimension and make some extensions to two-dimensional problems in which the interface lies along a coordinate direction. Fornberg and Meyer-Spasche [17] have considered elliptic equations with free boundaries that are solved on a uniform grid by adding correction terms near the interface to improve the accuracy.

Here we use a similar approach to derive modified difference equations for a quite general problem of the form (1.1), which produce second-order accurate results on a uniform grid in one or two dimensions. We derive appropriate coefficients at the grid points on a stencil that contains (in two dimensions) at most six points: the points of the standard five-point stencil plus a sixth point if we are near the interface, which is chosen from the set of diagonally adjacent grid points. The coefficients at these points can be determined by solving a system of six linear equations. The same approach should work in three dimensions as well and details will be presented elsewhere.

Instead of discontinuities in β, another possibility is that β is continuous but that the source term f has a delta function singularity along the interface Γ, e.g., in two dimensions

$$(1.2) \qquad f(x,y) = \int_\Gamma C(s)\, \delta(x - X(s))\, \delta(y - Y(s))\, ds,$$

where $(X(s), Y(s))$ is the arc-length parameterization of Γ and $C(s)$ is the source strength. By this we mean that $f(x,y)$ is a distribution with the property that

$$\int \int f(x,y)\phi(x,y)dxdy = \int_\Gamma C(s)\phi(X(s),Y(s))ds$$

for any smooth test function $\phi(x,y)$. Again the solution u will be continuous but the normal derivative will have a discontinuity of magnitude $C(s)$. As a model problem, consider the heat conduction problem in which a heat source is applied only along Γ. The temperature u will be highest along Γ, falling off to either side, resulting in a jump discontinuity in the normal derivative. In this case the standard five-point stencil can be used, but we must derive an appropriate term on the right-hand side to model the singular source. A dipole source may also occur, in which f contains the derivative of the delta function, and as a result the solution u itself is discontinuous across Γ. Again we can derive the appropriate right-hand side f_{ij} at each grid point so that the solution to the finite difference equations is second-order accurate in spite of the discontinuities.

More generally, we can handle discontinuities in β, κ, and f simultaneously with delta function or dipole sources. A general procedure for deriving the coefficients

in the stencil and the right-hand side is presented below. All that is required is a priori knowledge about the jumps in derivatives of u across Γ. For the above examples, sufficient information can be derived from the equation itself, without a priori knowledge of the solution.

Although this procedure is presented in the context of the elliptic equation (1.1), the same approach could be used for other problems where discontinuities in the solution or its derivatives are expected across immersed interfaces. A possible application would be to wave propagation through nonhomogeneous media with discontinuities in the propagation speed. This is currently being investigated.

Another potential application is to time-dependent parabolic equations where the elliptic part of the equation has the form (1.1). In this case Γ might be fixed (e.g., heat conduction in a nonhomogeneous material) or a moving free boundary governed by other equations coupled to the parabolic equation. The latter case arises in solidification problems, where Γ represents the interface between two phases of a substance, e.g., ice and water. In this case there is a discontinuity in the heat conduction coefficient across Γ and also a singular source at Γ due to latent heat release [11], [14]. Of course, this is a substantially more complicated problem, but an implicit method would require solving a Poisson problem of the above form in each time step. Mayo [19] disusses similar methods for the heat equation in irregular domains.

Another more complicated problem with similar characteristics arises in using the "immersed boundary method" to solve the incompressible Navier–Stokes equations in a region with complicated geometry. This method was originally developed by Peskin [23], [24] to model blood flow in the heart and has since been used for many other problems, particularly in biophysics [6], [12], [13], [15], [16]. The idea is to solve the Navier–Stokes equation on a uniform grid in a rectangular region in spite of the complicated time-varying geometry, e.g., the heart wall. This boundary is viewed as being immersed in the fluid and moves with the local fluid velocity. The boundary exerts force on the fluid, which is concentrated at the boundary, and hence gives a forcing term of the form (1.2) (although in this case u is a vector of velocities and $C(s)$ is a vector of force strengths in each coordinate direction). As a result the normal derivative of the tangential velocity will typically have a jump discontinuity at the interface and so will the pressure. The eventual development of second-order accurate methods for this problem was our original motivation in studying (1.1). We have called our general approach the *immersed interface method* since it is in the same spirit as Peskin's immersed boundary method but allows more general interface conditions.

Peskin's approach for the Navier–Stokes equations can be applied to problems of the form (1.1) as well, but only in the case of a delta function forcing term, not to problems with discontinuous coefficients. The main idea is to discretize the immersed boundary by a set of Lagrangian points $(X(s_k), Y(s_k))$, $k = 1, 2, \ldots, m$ and replace the integral in (1.2) by a discrete sum, also replacing the delta function by some discrete approximation $d_h(x)$ with support related to the mesh width h. Simple examples are the hat function

$$(1.3) \qquad d_h(x) = \begin{cases} (h - |x|)/h^2 & \text{if } |x| < h, \\ 0 & \text{if } |x| \geq h \end{cases}$$

and Peskin's discrete delta function

$$(1.4) \qquad d_h(x) = \begin{cases} \frac{1}{4h}\left(1 + cos(\frac{\pi x}{2h})\right) & \text{if } |x| < 2h, \\ 0 & \text{if } |x| \geq 2h. \end{cases}$$

In applying a finite difference method to (1.1) on a uniform grid we need values f_{ij} at (x_i, y_j). The value used is

$$(1.5) \qquad f_{ij} = \sum_{k=1}^{m} C(s_k)\, d_h(x_i - X_k)\, d_h(y_j - Y_k)\Delta s.$$

In one space dimension this approach is easy to analyze. In this case the interface reduces to a single point $x = \alpha \in (0, 1)$. For example, for the equation

$$(1.6) \qquad u''(x) = C\,\delta(x - \alpha), \qquad u(0) = u(1) = 0,$$

the solution is piecewise linear with a jump in the slope of magnitude C at $x = \alpha$. The finite difference method

$$(1.7) \qquad (u_{j+1} - 2u_j + u_{j-1})/h^2 = C\, d_h(x_j - \alpha)$$

with d_h given by (1.3) turns out to be very accurate; in fact it produces the exact solution $u = u(x_j)$ at all grid points in spite of the nonsmoothness of u (see [7]).

Beyer and LeVeque [7] have also analyzed time-dependent versions of the problem and show that second-order accuracy can still be obtained with an appropriate choice of the discrete delta function.

In two space dimensions, however, it does not appear to be possible to achieve second-order accuracy at all grid points using a right-hand side of the form (1.5). On the other hand, it turns out that the theoretical analysis used in [7] to analyze (1.7) can be extended to define numerical methods in two or three directions that are second order accurate, and this is the basis of the approach described below.

Work is currently underway to extend this approach to deal with time-varying boundaries, as, for example, in solidification problems or the incompressible Navier–Stokes equations. The focus here is on the elliptic equation (1.1). We note, however, that this will be required as a component of an eventual Navier–Stokes solver, since many methods for the incompressible Navier–Stokes equations require solving a Poisson problem for the pressure as a projection operation [4], [10]. The required jump in pressure across the interface can be imposed on the solution using our approach as described in §4.

1.1. Other approaches. At this point we should justify our interest in the use of uniform grids for problems of this nature. Using a grid that conforms to the interface is an obvious alternative, for example, a structured grid that is deformed in the neighborhood of the interface (e.g., [8]) or an unstructured triangulation. The finite element method on such a grid would be a natural choice for this elliptic equation and can be used very successfully (e.g., [3]). However, in many contexts the use of a uniform grid may be preferable.

In particular, if β is constant then we will see that the modified difference equation uses the standard five-point difference operator and only the right-hand side of the linear system is modified. This means that fast Poisson solvers can still be used to solve the system on a uniform grid, an advantage that would be lost on an irregular grid. Even if β is discontinuous so that the coefficients in the linear system must be

modified, the system maintains the same block structure as in the continuous case. We can then use available software designed to accept a user-specified stencil on a uniform rectangular grid.

More importantly, we are interested primarily in time-dependent problems, where a problem of the form (1.1) must be solved in each time step. In this case, the interface Γ is typically moving. Although it is possible to develop moving mesh methods that conform to Γ in each time step, this is generally much more complicated than simply allowing Γ to move relative to a fixed underlying uniform grid. For example, the immersed boundary method has been very successful in modeling flow in very complicated time-dependent geometries such as the beating heart with valves opening and closing. This would be difficult if not impossible to do with grids that conform to the boundary.

For problems with discontinuous coefficients, another approach to deriving the proper coefficients on a uniform grid stencil is the method of *harmonic averaging*. The one-dimensional expression $(\beta u_x)_x$, for example, can be approximated by

$$\frac{1}{h^2} \left[\beta_{i+1/2}(u_{i+1} - u_i) - \beta_{i-1/2}(u_i - u_{i-1}) \right].$$

If β is smooth then we can take $\beta_{i+1/2} = \beta(x_{i+1/2})$ (where $x_{i+1/2} = x_i + h/2$) and achieve second-order accuracy. If β is discontinuous in $[x_{i-1}, x_{i+1}]$, then the coefficients can be chosen as harmonic averages of $\beta(x)$, e.g.,

$$\beta_{i+\frac{1}{2}} = \left[\frac{1}{h} \int_{x_i}^{x_{i+1}} \beta^{-1}(x)\, dx \right]^{-1}.$$

This can be justified by homogenization theory for problems where $\beta(x)$ varies rapidly on the scale of the grid cells, and to some extent also for the case where β is simply discontinuous as we are considering, but the fact that this yields second-order accurate results seems to be primarily the result of fortuitous cancellation. In two space dimensions harmonic averaging is also commonly used to deal with discontinuous coefficients [5], [25], now integrating over squares to obtain the harmonic average of $\beta(x, y)$. In this case, however, the method does not appear to give second-order accurate results and we find that our approach is greatly superior.

2. One-dimensional problems. We begin by considering the one-dimensional problem

$$(2.1) \qquad\qquad (\beta u_x)_x + \kappa u = f + C\delta(x - \alpha)$$

on the interval $[0, 1]$ with specified boundary conditions on u at $x = 0$ and $x = 1$. The function $\beta(x)$ is allowed to be discontinuous at $x = \alpha$. For simplicity we will assume that $\kappa(x)$ and $f(x)$ are smooth functions, although discontinuities in these functions could also be handled with a minor modification of what follows.

We also allow an additional constraint to be imposed on the solution, namely, that the function u should have a jump discontinuity at $x = \alpha$ of specified strength $\hat{C}$,

$$(2.2) \qquad\qquad [u] = u^+ - u^- = \hat{C}.$$

This could be incorporated into (2.1) by including a dipole source term proportional to the derivative of the delta function, changing (2.1) to

$$(2.3) \qquad (\beta u_x)_x + \kappa u = f + C\delta(x - \alpha) + \tfrac{1}{2}(\beta^- + \beta^+)\hat{C}\delta'(x - \alpha).$$

For simplicity, however, we leave this as an external constraint.

By integrating (2.1) across the discontinuity, we find that βu_x has a jump of magnitude C,

$$(2.4) \qquad [\beta u_x] = \beta^+ u_x^+ - \beta^- u_x^- = C.$$

An alternative way to state the problem is to require that u satisfy the equation

$$(2.5) \qquad (\beta u_x)_x + \kappa u = f$$

in each of the intervals $(0, \alpha)$ and $(\alpha, 1)$, together with the two boundary conditions (2.2) and (2.4) at $x = \alpha$.

We now wish to approximate the solution $u(x)$ on a uniform grid in the interval $[0, 1]$, with

$$x_i = ih, \qquad i = 1, 2, \ldots, n,$$

where $h = 1/n$. The point α will typically fall between grid points, say $x_j \le \alpha < x_{j+1}$. Our goal is to develop finite difference equations of the form

$$(2.6) \qquad \gamma_{i,1} u_{i-1} + \gamma_{i,2} u_i + \gamma_{i,3} u_{i+1} + \kappa_i u_i = f_i + C_i, \qquad i = 1, 2, \ldots, n-1,$$

that can be used together with the boundary data u_0 and u_n to obtain a second-order accurate approximation to $u(x)$ at the uniform grid points.

For $i \ne j, j+1$ the solution u is smooth in the interval $[x_{i-1}, x_{i+1}]$ and we can use the standard approximation

$$(2.7) \qquad \frac{1}{h^2} \left(\beta_{i+1/2}(u_{i+1} - u_i) - \beta_{i-1/2}(u_i - u_{i-1}) \right) + \kappa_i u_i = f_i,$$

where

$$\beta_{i+1/2} = \beta(x_{i+1/2}), \quad \kappa_i = \kappa(x_i), \quad f_i = f(x_i).$$

In this case we can take

$$(2.8) \qquad \begin{aligned} \gamma_{i,1} &= \beta_{i-1/2}/h^2, \quad \gamma_{i,2} = -(\beta_{i-1/2} + \beta_{i+1/2})/h^2, \\ \gamma_{i,3} &= \beta_{i+1/2}/h^2, \quad \text{and} \quad C_i = 0. \end{aligned}$$

This gives a local truncation error that is $O(h^2)$:

$$(2.9) \qquad T_i = \gamma_{i,1} u(x_{i-1}) + \gamma_{i,2} u(x_i) + \gamma_{i,3} u(x_{i+1}) + \kappa_i u(x_i) - f_i = O(h^2).$$

We wish to determine formulas of the form (2.6) for $i = j$ and $i = j + 1$ so that second-order global accuracy is obtained. Since only two grid points are involved (independent of h), it is sufficient to have an $O(h)$ local truncation error at those points.

To compute the local truncation error at the point x_j, we expand u_{j-1}, u_j, and u_{j+1} in Taylor series about the point $x = \alpha$. Since we expect the γ coefficients to be $O(1/h^2)$ we must expand out through $O(h^3)$ to ensure an $O(h)$ truncation error. We use the notation

$$u^- = \lim_{x \to \alpha^-} u(x), \qquad u^+ = \lim_{x \to \alpha^+} u(x),$$

and expand to obtain

$$(2.10) \qquad u(x_{j-1}) = u^- + (x_{j-1} - \alpha)\, u_x^- + \tfrac{1}{2}(x_{j-1} - \alpha)^2\, u_{xx}^- + O(h^3),$$
$$(2.11) \qquad u(x_j) = u^- + (x_j - \alpha)\, u_x^- + \tfrac{1}{2}(x_j - \alpha)^2\, u_{xx}^- + O(h^3),$$
$$(2.12) \qquad u(x_{j+1}) = u^+ + (x_{j+1} - \alpha)\, u_x^+ + \tfrac{1}{2}(x_{j+1} - \alpha)^2\, u_{xx}^+ + O(h^3).$$

Note that if $x_j = \alpha$, then $u(x_j)$ is defined as the limit of the $u(x)$ approaching from the left. The corresponding u_j then is the approximation to this specific limit. We also use

$$(2.13) \qquad \kappa_j u(x_j) = \kappa(\alpha)\, u^-(\alpha) + O(h) \quad \text{and} \quad f_j = f(\alpha) + O(h).$$

The expression for $u(x_{j+1})$ involves $u^+, u_x^+,$ and u_{xx}^+ at α^+. However, using the known jump relations we can replace these by values at α^-. This will allow us to use the partial differential equation (PDE) (2.1) to determine the γ coefficients. From (2.2) and (2.4) we have

$$u^+ = u^- + \hat{C},$$
$$u_x^+ = (\beta^- u_x^- + C)/\beta^+.$$

From (2.5) we also see that $(\beta u_x)_x + \kappa u$ is continuous at $x = \alpha$, since f is, and so

$$\beta_x^+ u_x^+ + \beta^+ u_{xx}^+ + \kappa u^+ = \beta_x^- u_x^- + \beta^- u_{xx}^- + \kappa u^-$$

and hence

$$(2.14) \qquad u_{xx}^+ = \frac{1}{\beta^+}\left(\beta^- u_{xx}^- + \left(\beta_x^- - \frac{\beta_x^+ \beta^-}{\beta^+}\right) u_x^- - \frac{\beta_x^+}{\beta^+} C - \kappa\,\hat{C}\right).$$

Using these expressions in (2.12) gives

$$
\begin{aligned}
u(x_{j+1}) \;=\;& u^- + \left[\frac{\beta^-}{\beta^+}(x_{j+1} - \alpha) + \left(\frac{\beta_x^-}{\beta^+} - \frac{\beta_x^+ \beta^-}{(\beta^+)^2}\right)\frac{(x_{j+1} - \alpha)^2}{2}\right] u_x^- \\
(2.15) \qquad & + \frac{(x_{j+1} - \alpha)^2 \beta^-}{2\beta^+} u_{xx}^- + \hat{C} \\
& + (x_{j+1} - \alpha)\frac{C}{\beta^+} - \frac{(x_{j+1} - \alpha)^2}{2}\left(\frac{\beta_x^+}{\beta^+} C + \kappa\,\hat{C}\right).
\end{aligned}
$$

In computing the local truncation error we also use the PDE (2.1), which, in approaching α from the left, gives

$$(2.16) \qquad \beta_x^- u_x^- + \beta^- u_{xx}^- + \kappa(\alpha) u^- = f(\alpha).$$

We use this to replace the $f(\alpha)$ term in the local truncation error, obtaining

$$
\begin{aligned}
T_j \;=\;& \gamma_{j,1} u(x_{j-1}) + \gamma_{j,2} u(x_j) + \gamma_{j,3} u(x_{j+1}) + \kappa(\alpha) u^- \\
(2.17) \qquad & - [\beta_x^- u_x^- + \beta^- u_{xx}^- + \kappa u^-] - C_j + O(h).
\end{aligned}
$$

Replacing $u(x_{j-1}), u(x_j)$ and $u(x_{j+1})$ by the expressions (2.10)–(2.12) and collecting terms then gives

$$T_j = (\gamma_{j,1} + \gamma_{j,2} + \gamma_{j,3})u^- + \left\{ (x_{j-1} - \alpha)\gamma_{j,1} + (x_j - \alpha)\gamma_{j,2} \right.$$

$$(2.18) \quad + \left(\frac{\beta^-}{\beta^+}(x_{j+1} - \alpha) + \left(\frac{\beta_x^+}{\beta^+} - \frac{\beta_x^+\beta^-}{(\beta^+)^2} \right) \frac{(x_{j+1} - \alpha)^2}{2} \right) \gamma_{j3} - \beta_x^- \left. \right\} u_x^-$$

$$+ \frac{1}{2} \left\{ (x_{j-1} - \alpha)^2\gamma_{j,1} + (x_j - \alpha)^2\gamma_{j,2} + (x_{j+1} - \alpha)^2\frac{\beta^-}{\beta^+}\gamma_{j3} - 2\beta^- \right\} u_{xx}^-$$

$$+ \gamma_{j,3} \left\{ \hat{C} + (x_{j+1} - \alpha)\frac{C}{\beta^+} - \frac{(x_{j+1} - \alpha)^2}{2} \left(\frac{\beta_x^+C}{(\beta^+)^2} + \kappa\frac{\hat{C}}{\beta^+} \right) \right\} - C_j + O(h).$$

We can ensure that $T_j = O(h)$ by requiring that each coefficient of u^-, u_x^-, u_{xx}^- vanish, as well as the constant term. This gives four equations for the four unknowns $\gamma_{j,1}, \gamma_{j,2}, \gamma_{j,3}$, and C_j. The first three equations give a linear system for the γ's:

$$\gamma_{j,1} + \gamma_{j,2} + \gamma_{j,3} = 0,$$

$$(x_{j-1} - \alpha)\,\gamma_{j,1} + (x_j - \alpha)\,\gamma_{j,2}$$

$$(2.19) \quad + \left\{ \frac{\beta^-}{\beta^+}(x_{j+1} - \alpha) + \left(\frac{\beta_x^-}{\beta^+} - \frac{\beta^-\beta_x^+}{(\beta^+)^2} \right) \frac{(x_{j+1} - \alpha)^2}{2} \right\} \gamma_{j,3} = \beta_x^-,$$

$$\frac{(x_{j-1} - \alpha)^2}{2}\gamma_{j,1} + \frac{(x_j - \alpha)^2}{2}\gamma_{j,2} + \frac{(x_{j+1} - \alpha)^2}{2}\frac{\beta^-}{\beta^+}\gamma_{j,3} = \beta^-.$$

Once these γ's have been computed, we then set

$$(2.20) \quad C_j = \gamma_{j,3} \left\{ \hat{C} + (x_{j+1} - \alpha)\frac{C}{\beta^+} - \frac{1}{2}(x_{j+1} - \alpha)^2 \left(\frac{\beta_x^+C}{(\beta^+)^2} + \kappa\frac{\hat{C}}{\beta^+} \right) \right\}.$$

In a similar way, we can compute the coefficients in the equation at x_{j+1} from the system

$$\gamma_{j+1,1} + \gamma_{j+1,2} + \gamma_{j+1,3} = 0,$$

$$\left\{ \frac{\beta^+}{\beta^-}(x_j - \alpha) + \left(\frac{\beta_x^+}{\beta^-} - \frac{\beta_x^-\beta^+}{(\beta^-)^2} \right) \frac{(x_j - \alpha)^2}{2} \right\} \gamma_{j+1,1}$$

$$(2.21) \quad + (x_{j+1} - \alpha)\gamma_{j+1,2} + (x_{j+2} - \alpha)\gamma_{j+1,3} = \beta_x^+,$$

$$\frac{(x_j - \alpha)^2}{2}\frac{\beta^+}{\beta^-}\gamma_{j+1,1} + \frac{(x_{j+1} - \alpha)^2}{2}\gamma_{j+1,2} + \frac{(x_{j+2} - \alpha)^2}{2}\gamma_{j+1,3} = \beta^+,$$

and then

$$(2.22) \quad C_{j+1} = \gamma_{j+1,1} \left\{ -\hat{C} + (\alpha - x_j)\frac{C}{\beta^-} - \frac{1}{2}(\alpha - x_j)^2 \left(\frac{\beta_x^-C}{(\beta^-)^2} - \kappa\frac{\hat{C}}{\beta^-} \right) \right\}.$$

In the particular case when $\beta_x^- = 0$ and $\beta_x^+ = 0$ (in particular if β is piecewise constant), we can easily get explicit expressions for the γ_j's. Setting

$$D_j = h^2 + [\beta](x_{j-1} - \alpha)(x_j - \alpha)/2\beta^-,$$

$$D_{j+1} = h^2 - [\beta](x_{j+2} - \alpha)(x_{j+1} - \alpha)/2\beta^+,$$

these can be written as

$$\gamma_{j,1} = (\beta^- - [\beta](x_j - \alpha)/h)/D_j, \qquad \gamma_{j+1,1} = \beta^-/D_{j+1},$$

$$\gamma_{j,2} = (-2\beta^- + [\beta](x_{j-1} - \alpha)/h)/D_j, \quad \gamma_{j+1,2} = (-2\beta^+ + [\beta](x_{j+2} - \alpha)/h)/D_{j+1},$$

$$\gamma_{j,3} = \beta^+/D_j \qquad\qquad\qquad \gamma_{j+1,3} = (\beta^+ - [\beta](x_{j+1} - \alpha)/h)/D_{j+1},$$

provided that D_j, $D_{j+1} \neq 0$. In practical problems β often represents a physical quantity such as conductivity, permeability, or density and so $\beta > 0$ everywhere. In this case it is easy to show that each of the determinants D_j and D_{j+1} is also positive.

More generally, if $\beta^+\beta^- > 0$, then it can be shown that the systems (2.19) and (2.21) have unique solutions at least for all h sufficiently small, since the coefficients look essentially constant in a neighborhood of the point α on a fine enough grid.

If $\beta^+\beta^- < 0$ then the systems may be singular, although generically they are still nonsingular. Note that in this case it would be possible to multiply the equation by -1 on one side of α, yielding a problem with $\beta^-\beta^+ > 0$ at the possible expense of introducing discontinuities in κ and f. These discontinuities can easily be handled as described below. In this case we must be careful with the jump conditions; the jump conditions for the original equation must be imposed and not the jump conditions for the modified β.

Note also the following properties and special cases of the γ coefficients that result from solving these systems.

- The γ coefficients depend only on the function $\beta(x)$ and the position of α relative to the grid, and not on C or $\hat{C}$.
- If β is constant, then solving the systems (2.19) and (2.21) we recover the standard coefficients $\gamma_{i1} = \gamma_{i3} = \beta/h^2$ and $\gamma_{i2} = -2\beta/h^2$ for $i = j$, $j+1$.
- If β is continuous, then the standard coefficients (2.8) satisfy the system (2.19) to $O(h)$.
- In the case when β is piecewise constant, the harmonic averaging coefficients satisfy the first two equations of (2.19) but not the third, indicating that the truncation error of this method at x_j and x_{j+1} is $O(1)$. But we can prove that due to cancellation of errors this method is still second-order accurate.
- If $C = \hat{C} = 0$, then $C_j = C_{j+1} = 0$ and the inhomogeneous term in the difference equation is simply f_i. In this case a discontinuity in β affects only the coefficients and not the right-hand side.
- If β is constant and $\kappa = 0$, then

$$(2.23) \qquad C_j = \frac{1}{h^2}(x_{j+1} - \alpha)C + \frac{\beta}{h^2}\hat{C} = Cd_h(x_j - \alpha) + \hat{C}\beta d'_h(x_j - \alpha),$$

where d_h is the hat function (1.3). In this case we can view the difference scheme as a direct discretization of the equation

$$\beta u''(x) = f(x) + C\delta(x - \alpha) + \hat{C}\beta\delta'(x - \alpha).$$

2.1. The general one-dimensional problem. Now we suppose that f and κ may also have discontinuities at α. We only need a slight change in the linear systems for the γ_{jk}'s and $\gamma_{j+1,k}$'s and the corrections C_j and C_{j+1} to get the correct difference schemes at the grid points x_j, x_{j+1}.

At the grid point x_j, the first equation of the linear system (2.19) becomes

$$(2.24) \qquad \gamma_{j,1} + \gamma_{j,2} + \left(1 - \frac{(x_{j+1} - \alpha)^2}{2\beta+} [\kappa]\right) \gamma_{j,3} = 0$$

and the correction term now is

$$(2.25) \quad C_j = \gamma_{j,3} \left\{ \hat{C} + (x_{j+1} - \alpha) \frac{C}{\beta+} - \frac{(x_{j+1} - \alpha)^2}{2} \left(\frac{\beta_x^+ C}{(\beta^+)^2} + \kappa^+ \frac{\hat{C}}{\beta+} - \frac{[f]}{\beta+} \right) \right\}.$$

At the grid x_{j+1}, the first equation of the linear system (2.21) becomes

$$(2.26) \qquad \left(1 + \frac{(x_j - \alpha)^2}{2\beta-} [\kappa]\right) \gamma_{j+1,1} + \gamma_{j+1,2} + \gamma_{j+1,3} = 0$$

and the correction term is

$$(2.27) \quad C_{j+1} = \gamma_{j+1,1} \left\{ -\hat{C} + (\alpha - x_j) \frac{C}{\beta-} - \frac{(\alpha - x_j)^2}{2} \left(\frac{\beta_x^- C}{(\beta^-)^2} - \kappa^- \frac{\hat{C}}{\beta-} + \frac{[f]}{\beta-} \right) \right\}.$$

3. A simple two-dimensional problem. To introduce the ideas used in two dimensions in a simple framework, we begin by considering the equation

$$(3.1) \qquad (\beta u_x)_x + (\beta u_y)_y + \kappa(x,y) u = f(x,y), \qquad (x,y) \in \Omega$$

in the case where β is piecewise constant and has a jump discontinuity across some curve Γ in Ω, while κ and f are assumed to be smooth. Formulas for the more general case, in which κ and f may be discontinuous, f may contain singular forces, and we may also require a discontinuity in the solution u, will be presented in §4.

The interface Γ can be an arbitrary piecewise smooth curve lying in Ω. We need not assume that Γ is closed or even connected. It may consist of several segments.

We assume the domain Ω is a square, say $[a,b] \times [a,b]$. We take a uniform grid with

$$x_i = a + ih, \quad y_j = a + jh, \quad i,j = 0,1,\ldots,n,$$

where $h = (b-a)/n$. Figure 1 gives an example of the uniform grid and the immersed interface.

Our goal is to develop a finite difference equation of the form

$$(3.2) \qquad \sum_k \gamma_k u_{i+i_k, j+j_k} + \kappa_{ij} u_{ij} = f_{ij} + C_{ij}$$

for use at the point (x_i, y_j). The sum over k involves a finite numbers of points neighboring (x_i, y_j) (at most six in the formula we derive). So each i_k, j_k will take values in the set $\{-1, 0, 1\}$. The coefficients γ_k and indices i_k, j_k will depend on (i,j), so these should really be labeled γ_{ijk}, etc., but for simplicity of notation we will concentrate on a single point (i,j) and drop these indices.

We say (i,j) is a *regular point* if the interface does not come between any points in the standard five-point stencil centered at (i,j). At these points we obtain an $O(h^2)$ truncation error using the standard 5-point ($k = 5$) formula

$$(3.3) \quad \frac{1}{h} \left(\left(\beta_{i+1/2,j} \frac{(u_{i+1,j} - u_{ij})}{h} - \beta_{i-1/2,j} \frac{(u_{ij} - u_{i-1,j})}{h} \right) \right.$$
$$\left. + \left(\beta_{i,j+1/2} \frac{(u_{i,j+1} - u_{i,j})}{h} - \beta_{i,j-1/2} \frac{(u_{i,j} - u_{i,j-1})}{h} \right) \right) + \kappa_{ij} u_{ij} = f_{ij},$$
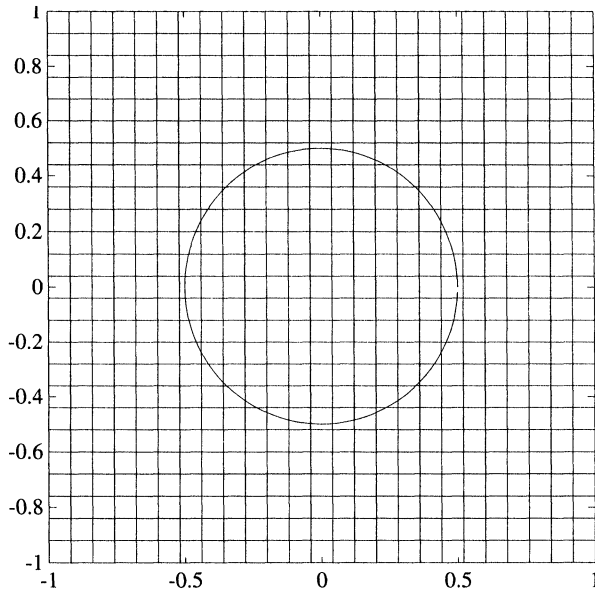
FIG. 1. *A circular interface* Γ *in a* 26×26 *uniform grid. This geometry is used for the test problems presented in* §5.
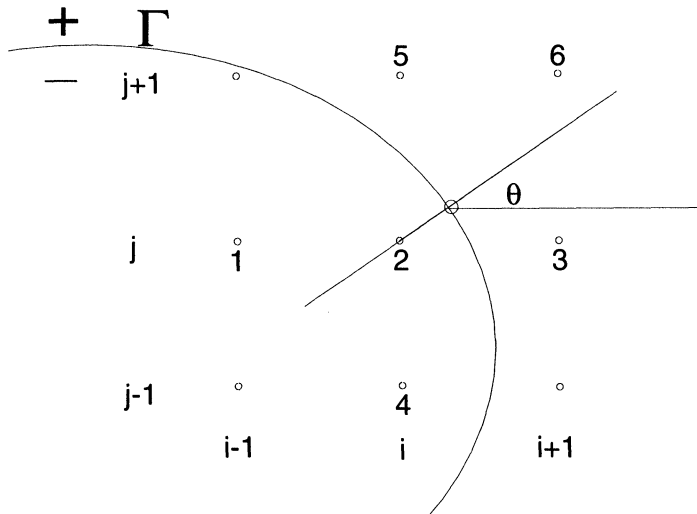

FIG. 2. *The geometry at an irregular grid point* (i, j). *The coefficients* γ_1 *through* γ_6 *will be determined for the stencil points labelled 1–6. The circled point on* Γ *is the point* (x_i^*, y_j^*).

with

$$(3.4) \qquad\qquad C_{ij} = 0.$$

We wish to determine formulas of the form (3.2) for the irregular points also. Since these points are adjacent to the curve Γ and form a lower-dimensional set, it turns out to be sufficient to require an $O(h)$ truncation error at these points, just as in one dimension. We follow the same approach as in one dimension and expand all

the $u_{i+i_k,j+j_k}$ about some point (x_i^*, y_j^*) on the interface Γ. In one dimension there was only one such point, α. In two dimensions we have flexibility in choosing (x_i^*, y_j^*). We might take, for example, the point closest to (x_i, y_j) as illustrated in Fig. 2. We then expand each $u_{i+i_k,j+j_k}$ about (x_i^*, y_j^*), being careful to use the limiting values of derivatives of u from the correct side of the interface. We use the superscripts $-$ or $+$ to denote the limiting values of a function from one side or the other. As an example, in the configuration shown in Fig. 2, we would expand

$$
\begin{aligned}
u(x_i, y_j) \;=\; & u^- + u_x^- \, (x_i - x_i^*) + u_y^- \, (y_j - y_j^*) + \tfrac{1}{2} u_{xx}^- \, (x_i - x_i^*)^2 \\
& + \tfrac{1}{2} u_{yy}^- \, (y_j - y_j^*)^2 + u_{xy}^- \, (x_i - x_i^*)(y_j - y_j^*) + O(h^3)
\end{aligned}
$$
(3.5)

and

$$
\begin{aligned}
u(x_{i+1}, y_j) \;=\; & u^+ + u_x^+ \, (x_{i+1} - x_i^*) + u_y^+ \, (y_j - y_j^*) + \tfrac{1}{2} u_{xx}^+ \, (x_{i+1} - x_i^*)^2 \\
& + \tfrac{1}{2} u_{yy}^+ \, (y_j - y_j^*)^2 + u_{xy}^+ \, (x_{i+1} - x_i^*)(y_j - y_j^*) + O(h^3).
\end{aligned}
$$
(3.6)

If we do this expansion at each point used in the difference equation (3.2) then the local truncation error T_{ij} can be expressed as a linear combination of the values $u^\pm, u_x^\pm, u_y^\pm, u_{xx}^\pm, u_{xy}^\pm, u_{yy}^\pm$. Following the one-dimensional derivation in §2, we now wish to eliminate all values on one side of the interface, say the values $u^+, u_x^+, u_y^+, u_{xx}^+, u_{xy}^+,$ u_{yy}^+, in terms of the values on the other side, $u^-, u_x^-, u_y^-, u_{xx}^-, u_{xy}^-, u_{yy}^-$. We must do this using the jump conditions across Γ,

$$
u^- = u^+
$$
(3.7)

and

$$
\beta^- \frac{\partial u^-}{\partial n} = \beta^+ \frac{\partial u^+}{\partial n},
$$
(3.8)

where $\partial/\partial n$ represents differentiation in the normal direction. From (3.7) we have that tangential derivatives are continuous, while (3.8) gives information about the jump in the normal direction. Differentiating these and manipulating the results allows us to perform the desired elimination, as detailed below. To do this, it turns out to be very convenient to first perform a local coordinate transformation into directions ξ, normal to Γ, and η, tangential to Γ.

Once T_{ij} is expressed as a linear combination of the values $u^-, u_x^-, u_y^-, u_{xx}^-, u_{xy}^-,$ and u_{yy}^-, we must require that the coefficient of each of these terms vanishes to achieve an $O(h)$ truncation error. This gives a linear system of six equations to determine the coefficients γ_k. To obtain a solvable system we require six points in the stencil. We use the standard five-point stencil together with one additional point.

To summarize, to determine the difference scheme at an irregular grid point we need to take the following steps.

- Select a point $(x_i^*, y_j^*) \in \Gamma$ near (x_i, y_j).
- Apply a local coordinate transformation in directions normal and tangential to Γ at (x_i^*, y_j^*).
- Derive the jump conditions relating $+$ and $-$ values at (x_i^*, y_j^*) in the local coordinates.
- Choose an additional point to form a six–point stencil.
- Set up and solve a linear system of six equations for the coefficients γ_k. The value C_{ij} is also obtained.

Below we give a detailed analysis of each step.

For each irregular grid point (x_i, y_j) we need to find a point (x_i^*, y_j^*) on the interface. We usually take this point as the projection of (x_i, y_j) on the interface if the interface is smooth at this point. Otherwise we can take any smooth point on the interface in the neighborhood of (x_i, y_j). In some contexts it may be more convenient to choose a nearby point that lies on a coordinate line between (x_i, y_j) and one of its neighbors.

After choosing (x_i^*, y_j^*) we are ready to apply a local coordinate transformation (shift + rotation) near this grid point. Let θ be the angle between the x-axis and the normal direction, pointing in the direction of the $+$ side. The transformation is as follows:

$$(3.9) \qquad \xi = (x - x_i^*)\cos\theta + (y - y_j^*)\sin\theta,$$

$$(3.10) \qquad \eta = -(x - x_i^*)\sin\theta + (y - y_j^*)\cos\theta.$$

Note that under this local coordinate transformation the PDE (3.1) remains unchanged. In fact, this is true more generally when β, κ, and f depend on x and y, as is shown in §4. We should have new notation for $u(x, y), \kappa(x, y), f(x, y)$ in the local coordinates, say, $\bar{u}(\xi, \eta) = u(x, y)$, $\bar{\kappa}(\xi, \eta) = \kappa(x, y)$, and $\bar{f}(\xi, \eta) = f(x, y)$. For simplicity we drop the bars and use the same notation in the local coordinates as in the old ones. With these local coordinates we are able to derive the interface conditions as we did in §2.

3.1. The interface relations in the local coordinates for two-dimensional problems. We consider a fixed point (x_i^*, y_j^*) and define a new ξ-η coordinate system based on the directions normal and tangential to Γ at this point using the formulas (3.9) and (3.10). In a neighborhood of this point, the interface lies roughly in the η-direction, so we can parameterize Γ locally by $\xi = \chi(\eta), \eta = \eta$. Note that $\chi(0) = 0$ and, provided the boundary is smooth at (x_i^*, y_j^*), $\chi'(0) = 0$ as well.

The continuity condition (3.7) holds at each point on Γ. In our local coordinates, we can write this as

$$(3.11) \qquad u^-(\chi(\eta), \eta) = u^+(\chi(\eta), \eta)$$

for all η in a neighborhood of $\eta = 0$. Differentiating this with respect to η gives

$$(3.12) \qquad u_\xi^- \chi' + u_\eta^- = u_\xi^+ \chi' + u_\eta^+$$

or, in compact form,

$$(3.13) \qquad [u_\xi]\chi' + [u_\eta] = 0.$$

Differentiating again with respect to η gives

$$(3.14) \qquad [u_{\xi\xi}]\chi'^2 + 2[u_{\xi\eta}]\chi' + [u_\xi]\chi'' + [u_{\eta\eta}] = 0.$$

Evaluating (3.13) and (3.14) at $\eta = 0$, where $\chi' = 0$, gives two of the desired jump conditions:

$$(3.15) \qquad [u_\eta] = 0, \quad \text{i.e.,} \quad u_\eta^- = u_\eta^+ = u_\eta,$$

$$(3.16) \qquad [u_\xi] \chi'' + [u_{\eta\eta}] = 0.$$

We also have the jump condition (3.8) at each point on Γ. At a point $(\chi(\eta), \eta) \in \Gamma$ we can express the normal derivative in terms of ξ- and η- derivatives as

$$\frac{\partial u}{\partial n} = \frac{1}{\sqrt{1 + \chi'^2}} \left(u_\xi - u_\eta \chi' \right)$$

so that we can write (3.8) as

(3.17) $$\beta^- (u_\xi^- - u_\eta^- \chi') = \beta^+ (u_\xi^+ - u_\eta^+ \chi').$$

Differentiating this with respect to η gives

(3.18) $$\left[\beta \left(u_{\xi\xi} \chi' + u_{\xi\eta} - u_\eta \chi'' - u_{\xi\eta} \chi'^2 - u_{\eta\eta} \chi' \right) \right] = 0.$$

Evaluating (3.17) and (3.18) at $\eta = 0$ gives more jump conditions:

(3.19) $$[\beta u_\xi] = 0,$$

(3.20) $$[\beta (u_{\xi\eta} - u_\eta \chi'')] = 0.$$

We can use the relations (3.17)–(3.20) to derive the following expressions for values on the $+$ side of Γ in terms of values in the $-$ side. Setting

$$\rho = \beta^- / \beta^+,$$

we can write these relations as

(3.21)
$$u^+ = u^-,$$
$$u_\eta^+ = u_\eta^-,$$
$$u_\xi^+ = \rho u_\xi^-,$$
$$u_{\xi\eta}^+ = \rho u_{\xi\eta}^- + (1 - \rho)\, u_\eta^- \chi'',$$
$$u_{\eta\eta}^+ = u_{\eta\eta}^- + (1 - \rho)\, u_\xi^- \chi''.$$

To obtain an expression for $u_{\xi\xi}^+$, we note that the PDE (3.1) gives

$$\beta^+ u_{\xi\xi}^+ = \beta^- u_{\xi\xi}^- + \beta^- u_{\eta\eta}^- - \beta^+ u_{\eta\eta}^+$$

so that

(3.22) $$u_{\xi\xi}^+ = \rho u_{\xi\xi}^- + (\rho - 1) u_{\eta\eta}^- + (\rho - 1) u_\xi^- \chi''.$$

Now we have expressed all the quantities with $(+)$ superscripts in terms of the quantities with $(-)$ superscripts for the case $\chi'(0) = 0$. In this simple case they are homogeneous. The next thing to do is to choose an additional point from $(i - 1, j - 1), (i-1, j+1), (i+1, j-1), (i+1, j+1)$ in addition to the standard five-point stencil. It seems that the best choice is the point that has the shortest distance from (x^*, y^*). The additional point can be written as (x_{i+i_0}, y_{j+j_0}), where i_0 and j_0 are each -1 or 1 depending on the position of the additional point.

3.2. The derivation of the difference scheme for an irregular point. We are now ready to derive the difference schemes at irregular grid points. Denote the ξ-η coordinates of the six points in the difference stencil,

$$(x_{i-1}, y_j), (x_i, y_j), (x_{i+1}, y_j), (x_i, y_{j-1}), (x_i, y_{j+1}), (x_{i+i_0}, y_{j+j_0}),$$

as

$$(\xi_1, \eta_1), (\xi_2, \eta_2), (\xi_3, \eta_3), (\xi_4, \eta_4), (\xi_5, \eta_5), (\xi_6, \eta_6),$$

respectively. The local truncation error T_{ij} of the difference scheme (3.2) at (x_i, y_j) is then

$$(3.23) \qquad \begin{aligned} T_{ij} = {} & \gamma_1 u(\xi_1, \eta_1) + \gamma_2 u(\xi_2, \eta_2) + \gamma_3 u(\xi_3, \eta_3) + \gamma_4 u(\xi_4, \eta_4) \\ & + \gamma_5 u(\xi_5, \eta_5) + \gamma_6 u(\xi_6, \eta_6) + \kappa_{ij} u(\xi_2, \eta_2) - f_{ij} - C_{ij}. \end{aligned}$$

We now expand all the terms about $(0, 0)$ in the local coordinates from each side of the interface, as we did in (3.5) and (3.6), obtaining

$$u(\xi_k, \eta_k) = u^{\pm} + \xi_k u_{\xi}^{\pm} + \eta_k u_{\eta}^{\pm} + \tfrac{1}{2} \xi_k^2 u_{\xi\xi}^{\pm} + \xi_k \eta_k u_{\xi\eta}^{\pm} + \tfrac{1}{2} \eta_k^{\pm} u_{\eta\eta}^{\pm} + O(h^3),$$

where the $+$ or $-$ sign is chosen depending on whether (ξ_k, η_k) lies on the $+$ or $-$ side of Γ.

We also use

$$(3.24) \qquad \kappa_{ij} u(\xi_2, \eta_2) = \kappa^{-} u^{-} + O(h) \quad \text{and} \quad f_{ij} = f^{-} + O(h),$$

where $\kappa^{-} = \kappa(0, 0)$ and so forth (recall that $\kappa, u,$ and f are continuous). Using these expansions in (3.23) and collecting terms gives an expression of the form

$$(3.25) \qquad \begin{aligned} T_{ij} = {} & a_1 u^{-} + a_2 u^{+} + a_3 u_{\xi}^{-} + a_4 u_{\xi}^{+} + a_5 u_{\eta}^{-} + a_6 u_{\eta}^{+} + a_7 u_{\xi\xi}^{-} + a_8 u_{\xi\xi}^{+} \\ & + a_9 u_{\eta\eta}^{-} + a_{10} u_{\eta\eta}^{+} + a_{11} u_{\xi\eta}^{-} + a_{12} u_{\xi\eta}^{+} + \kappa^{-} u^{-} - f^{-} - C_{ij} + O(h). \end{aligned}$$

The coefficients a_j depend only on the position of the stencil relative to the interface. They are independent of the functions $u, \kappa,$ and f. If we define the index sets K^+ and K^- by

$$K^{\pm} = \{k : (\xi_k, \eta_k) \text{ is on the } \pm \text{ side of } \Gamma\},$$

then the a_j are given by

$$(3.26) \qquad \begin{aligned} a_1 &= \sum_{k \in K^-} \gamma_k, & a_2 &= \sum_{k \in K^+} \gamma_k, \\ a_3 &= \sum_{k \in K^-} \xi_k \gamma_k, & a_4 &= \sum_{k \in K^+} \xi_k \gamma_k, \\ a_5 &= \sum_{k \in K^-} \eta_k \gamma_k, & a_6 &= \sum_{k \in K^+} \eta_k \gamma_k, \\ a_7 &= \frac{1}{2} \sum_{k \in K^-} \xi_k^2 \gamma_k, & a_8 &= \frac{1}{2} \sum_{k \in K^+} \xi_k^2 \gamma_k, \\ a_9 &= \frac{1}{2} \sum_{k \in K^-} \eta_k^2 \gamma_k, & a_{10} &= \frac{1}{2} \sum_{k \in K^+} \eta_k^2 \gamma_k, \\ a_{11} &= \sum_{k \in K^-} \xi_k \eta_k \gamma_k, & a_{12} &= \sum_{k \in K^+} \xi_k \eta_k \gamma_k. \end{aligned}$$

Using the interface relations (3.21) and (3.22) in (3.25) and rearranging it we obtain

$$
\begin{aligned}
T_{ij} = {} & (a_1 + a_2)\, u^- + \left\{ a_3 + a_4\,\rho + a_8\,(\rho - 1)\,\chi'' + a_{10}\,(1 - \rho)\,\chi'' \right\} u_\xi^- \\
& + \left\{ a_5 + a_6 + a_{12}\,(1 - \rho)\,\chi'' \right\} u_\eta^- + \left\{ a_7 + a_8\rho - \beta^- \right\} u_{\xi\xi}^- \\
& + \left\{ a_9 + a_{10} + a_8\,(\rho - 1) - \beta^- \right\} u_{\eta\eta}^- + \left\{ a_{11} + a_{12}\rho \right\} u_{\xi\eta}^- \\
& + \left\{ \beta^-\,(u_{\xi\xi}^- + u_{\eta\eta}^-) + k^-\,u^- - f^- + C_{ij} \right\} + O(h),
\end{aligned}
$$

(3.27)

where again $\rho = \beta^- / \beta^+$. From the PDE (2.1) we know that

$$
\beta^-\,(u_{\xi\xi}^- + u_{\eta\eta}^-) + k^-\,u^- - f^- = 0
$$

and so this term drops out of (3.27) by taking $C_{ij} = 0$. We can ensure that $T_{ij} = O(h)$ by requiring that each coefficient of $u^-, u_\xi^-, u_\eta^-, u_{\xi\xi}^-, u_{\xi\eta}^-$, and $u_{\eta\eta}^-$ vanish. This gives six equations for the six unknowns $\gamma_1, \cdots, \gamma_6$:

$$
\begin{aligned}
a_1 + a_2 &= 0, \\
a_3 + a_4\,\rho + a_8\,(\rho - 1)\,\chi'' + a_{10}\,(1 - \rho)\,\chi'' &= 0, \\
a_5 + a_6 + a_{12}\,(1 - \rho)\,\chi'' &= 0, \\
a_7 + a_8\,\rho &= \beta^-, \\
a_9 + a_{10} + a_8\,(\rho - 1) &= \beta^-, \\
a_{11} + a_{12}\,\rho &= 0.
\end{aligned}
$$

(3.28)

As in one dimension, if $\beta^- \beta^+ > 0$, then the linear system has a unique solution. To prove this is not very complicated but rather tedious. We need to consider all the possible cases for the formation of the new stencil (i.e., the position of the points relative to the interface). We omit the detailed analysis here. If $\beta^- \beta^+ < 0$, then it turns out that only for some specific value of $[\beta]$ is the coefficient matrix for the unknown γ_j's singular, so the algorithm is typically successful even in this case. Moreover, by negating the equation on one side of the interface, it is possible to insure that $\beta^- \beta^+ > 0$ at the expense of perhaps introducing discontinuities into κ and f.

Note that since the interface relations (3.21) and (3.22) are homogenous, we have $C_{ij} = 0$ and there is no contribution to the right-hand side resulting from the discontinuous coefficients. If $\beta^+ = \beta^-$ then solving (3.28) we recover the standard five-point coefficients

$$
\gamma_1 = \gamma_3 = \gamma_4 = \gamma_5 = \beta/h^2, \quad \gamma_2 = -4\beta/h^2, \quad \text{and} \quad \gamma_6 = 0.
$$

In general, however, the resulting γ_j's are different from those in the standard five-point stencil. Figure 3 shows some representative stencils for a problem in which β has the value 1 on one side of Γ and 3 on the other side.

The exact nature of the coefficients depends on how large the jump in β is. We have not investigated these coefficients in general, but at least for reasonably mild discontinuities we can make the following assumptions.

- The contributions to the difference schemes at irregular points are mainly from the standard five-point stencil. These coefficients are $O(1/h^2)$ while the contributions from the "additional points" are typically much smaller. The magnitude depends on the jump in β and the geometry of the grid.
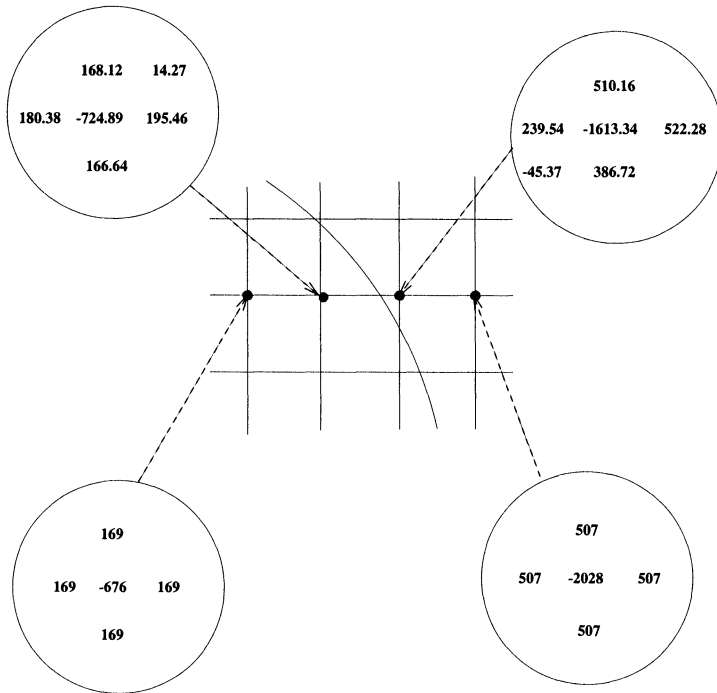
FIG. 3. *The γ_j coefficients at four grid points near the interface. The coefficient β is piecewise constant with the value $\beta = 1$ to the left and $\beta = 3$ to the right. The standard five-point stencil is used at regular grid points while special six-point stencils are used near the interface. The grid is a section of Fig. 1, with $h = 1/13$.*

- All the coefficients except occasionally γ_6 have the same sign ($-$ for the diagonal and $+$ for the off-diagonal) as in the classic five-point difference formula. Since the contribution from the sixth point is much smaller than from the standard five points, we expect the classical theoretical analysis to still be applicable for the resulting linear system with slight modifications. In particular, the system is nearly diagonally dominant, and strictly so if γ_6 is always positive.

We use an iterative method to solve the resulting linear system, which is block tridiagonal. In most of our numerical experiments we have used a line successive over-relaxation (LSOR) iteration. If $\beta^- \beta^+ > 0$, the relaxation parameter is chosen as the optimal parameter for the Poisson problem on a square. The convergence speed is almost the same as that if we use the LSOR method to solve the Poisson problem with constant β on a square. This confirms the conclusions above. However, if $\beta^- \beta^+ < 0$, it is difficult to determine a suitable relaxation parameter and we simply use line Gauss–Seidel iteration. Since this case is less interesting physically, we have not investigated other approaches.

In the future, we plan to study the use of multigrid methods to achieve faster convergence. It is not clear how the multigrid convergence rate will be affected by the discontinuity in the coefficients. Multigrid methods for problems like (3.1) with discontinuous coefficients have been previously studied (e.g., [1], [9]), but mainly for problems where the interfaces are aligned with the coordinate directions.

4. The general two-dimensional problem. In this section we present the analysis for the more complicated two-dimensional problem

$$(4.1) \qquad (\beta\, u_x\,)_x + (\beta\, u_y\,)_y + \kappa(x,y)\, u = f(x,y), \qquad (x,y) \in \Omega.$$

Now β, κ, and f may all have discontinuities along a general interface Γ, and so do $u, u_x, u_y, u_{xx}, u_{xy}$, and u_{yy}. The process basically is the same as in the discussion of §3. We use the same notation and assumptions about the region Ω, uniform grid, and arbitrary interface Γ. Again we want to use the difference scheme (3.2). For regular grid points, we still apply the standard five-point stencil (3.3) and (3.4), giving a local truncation error of $O(h^2)$. We will concentrate on the derivation of the difference scheme at a typical irregular point (x_i, y_j).

We first demonstrate that the PDE (4.1) remains unchanged if the coordinate transformation is composed of a shift and rotation. In fact, taking an arbitrary function $w(x,y)$, under the transformations (3.9) and (3.10), we have

$$w_x = \bar{w}_\xi \cos\theta - \bar{w}_\eta \sin\theta,$$
$$w_y = \bar{w}_\xi \sin\theta + \bar{w}_\eta \cos\theta,$$

where $\bar{w}(\xi, \eta) = w(x,y)$ and so forth, so we have

$$
\begin{aligned}
(\beta\, u_x)_x + (\beta\, u_y)_y + \kappa u &= \beta\, (u_{xx} + u_{yy}) + \beta_x\, u_x + \beta_y\, u_y + \kappa u \\
&= \bar{\beta}\, (\bar{u}_{\xi\,\xi} + \bar{u}_{\eta\,\eta}) + (\bar{\beta}_\xi \cos\theta - \bar{\beta}_\eta \sin\theta)\, (\bar{u}_\xi \cos\theta - \bar{u}_\eta \sin\theta) \\
&\quad + (\bar{\beta}_\xi \sin\theta + \bar{\beta}_\eta \cos\theta)\, (\bar{u}_\xi \sin\theta + \bar{u}_\eta \cos\theta) + \bar{\kappa}\bar{u} \\
&= \bar{\beta}\, (\bar{u}_{\xi\,\xi} + \bar{u}_{\eta\,\eta}) + \bar{\beta}_\xi\, \bar{u}_\xi + \bar{\beta}_\eta\, \bar{u}_\eta + \bar{\kappa}\bar{u} \\
&= (\bar{\beta}\, \bar{u}_\xi)_\xi + (\bar{\beta}\, \bar{u}_\eta)_\eta + \bar{\kappa}\bar{u}.
\end{aligned}
$$

For simplicity, we will drop the bars again. If some grid point $u(x_i, y_j)$ happens to fall on the interface, then $u(x_i, y_j)$ is defined as the limiting value of $u(x,y)$ from one side of the interface or other. The same argument applies to all other functions such as β, κ, f and the derivatives of $u(x,y)$. The corresponding u_{ij} is the approximation to this specific limit. We again use the superscripts $-$ and $+$ to express the limiting values from one side of the interface or the other.

The essential difference now is that the interface relations are more complicated. Two interface conditions are needed in advance to make the problem well-posed. We assume locally that they are defined by

$$(4.2) \qquad u^+ - u^- = w(\eta),$$

$$(4.3) \qquad \beta^+ \frac{\partial u^+}{\partial n} - \beta^- \frac{\partial u^-}{\partial n} = v(\eta),$$

where again $\xi = \chi(\eta)$, $\eta = \eta$ is the parametric representation of the interface in the neighborhood of the point (x_i^*, y_j^*). Here $v(\eta)$ and $w(\eta)$ are arbitrary (smooth) functions that are used to impose quite general jump conditions across Γ. (Often $v = w = 0$, but we may wish to impose other jumps as an external constraint. An example occurs in the incompressible Navier–Stokes equations with the immersed boundary method, where the known jump in pressure across the interface must be imposed in the solution of a Poisson problem.)

Differentiating (4.2) with respect to η along the interface we obtain

$$(4.4) \qquad [u_\xi]\, \chi' + [u_\eta] = w'(\eta).$$

Differentiating this again with respect to η we obtain

$$(4.5) \qquad [u_\xi] \, \chi'' + \chi' \frac{d}{d\eta} [u_\xi] + [u_{\xi\eta}] \, \chi' + [u_{\eta\eta}] = w''(\eta).$$

Note that in the local coordinates, (4.3) can be written as

$$(4.6) \qquad \beta^+ (u_\xi^+ - u_\eta^+ \chi') = \beta^- (u_\xi^- - u_\eta^- \chi') + v\sqrt{1 + (\chi')^2}.$$

Differentiating this with respect to η along the interface we have

$$
\begin{aligned}
(\beta_\xi{}^+ \chi' + \beta_\eta{}^+) \, (u_\xi^+ - u_\eta^+ \chi') &+ \beta^+ \left(u_{\xi\xi}^+ \chi' + u_{\xi\eta}^+ - \frac{d}{d\eta}(u_\eta^+) \, \chi' - u_\eta^+ \chi'' \right) \\
&= (\beta_\xi^- \chi' + \beta_\eta^-) \, (u_\xi^- - u_\eta^- \chi') \\
(4.7) \qquad &\quad + \beta^- \left(u_{\xi\xi}^- x' + u_{\xi\eta}^- - \frac{d}{d\eta}(u_\eta^-) \, \chi' - u_\eta^- \chi'' \right) \\
&\quad + v'(\eta) \left(\sqrt{1 + (\chi')^2} + \frac{v(\eta)\chi'\chi''}{\sqrt{1 + (\chi')^2}} \right).
\end{aligned}
$$

Also from the PDE we know that

$$
\begin{aligned}
(4.8) \qquad u_{\xi\xi}^+ &= \frac{\beta^-}{\beta^+} u_{\xi\xi}^- + \frac{\beta^-}{\beta^+} u_{\eta\eta}^- - u_{\eta\eta}^+ + \frac{\beta_\xi^-}{\beta^+} u_\xi^- - \frac{\beta_\xi^+}{\beta^+} u_\xi^+ \\
&\quad + \frac{\beta_\eta^-}{\beta^+} u_\eta^- - \frac{\beta_\eta^+}{\beta^+} u_\eta^+ + \frac{[f]}{\beta^+} + \frac{\kappa^- u^- - \kappa^+ u^+}{\beta^+}.
\end{aligned}
$$

The numerator of the last term can be rewritten as

$$(4.9) \qquad \kappa^- u^- - \kappa^+ u^+ = -[\kappa] \, u^- - [u] \, \kappa^+.$$

Using these relations, we can express quantities with $(+)$ superscripts in terms of those with $(-)$ superscripts. The detailed analysis is similar to the process in §3, although it is more complicated due to the fact that $\beta(x, y)$ is not constant in the neighborhood of the interface and the presence of the source-like terms $w(\eta)$, $v(\eta)$. To save space here we omit the detailed analysis and simply present the results. Recall that the parameterization $\xi = \chi(\eta)$ is assumed to be smooth with $\chi'(0) = 0$ and that we are considering the jumps across Γ at a fixed point (x_i^*, y_j^*) corresponding to $\xi = \eta = 0$. In the expressions below, all functions are evaluated at this point. The jump relations are given by

$$
\begin{aligned}
u^+ &= u^- + w, \\
u_\xi^+ &= \rho \, u_\xi^- + \frac{v}{\beta^+}, \\
u_\eta^+ &= u_\eta^- + w', \\
(4.10) \qquad u_{\xi\xi}^+ &= \left(\frac{\beta_\xi^-}{\beta^+} - \chi'' \right) u_\xi^- + \left(\chi'' - \frac{\beta_\xi^+}{\beta^+} \right) u_\xi^+ + \frac{\beta_\eta^-}{\beta^+} u_\eta^- - \frac{\beta_\eta^+}{\beta^+} u_\eta^+ \\
&\quad + (\rho - 1) u_{\eta\eta}^- + \rho u_{\xi\xi}^- - w'' + \frac{[f]}{\beta^+} - \frac{[\kappa] \, u^- + \kappa^+ [u]}{\beta^+} \\
u_{\eta\eta}^+ &= u_{\eta\eta}^- + (u_\xi^- - u_\xi^+) \, \chi'' + w'', \\
u_{\xi\eta}^+ &= \frac{\beta_\eta^-}{\beta^+} u_\xi^- - \frac{\beta_\eta^+}{\beta^+} u_\xi^+ + (u_\eta^+ - \rho u_\eta^-) \, \chi'' + \rho \, u_{\xi\eta}^- + \frac{v'}{\beta^+}.
\end{aligned}
$$

The local truncation error T_{ij} at (x_i, y_j) is again given by (3.25) with the coefficients a_k given by the expressions (3.26) in terms of the unknowns γ_k. We now replace all of the $(+)$ values by expressions involving $(-)$ values using (4.10). After combining common terms and eliminating some terms due to the relation

$$\beta^- \left(u_{\xi\xi}^- + u_{\eta\eta}^- \right) + \beta_\xi^- u_\xi^- + \beta_\eta^- u_\eta^- + k^- u^- - f^- = 0$$

(resulting from the PDE (4.1)), we obtain

$$T_{ij} = \left(a_1 - \frac{a_8\,[\kappa]}{\beta^+} + a_2 \right) u^- + \left\{ a_3 + a_8 \left(\frac{\beta_\xi^-}{\beta^+} - \chi'' \right) + a_{10}\chi'' + a_{12}\frac{\beta_\eta^-}{\beta^+} \right.$$

$$\left. + \rho \left(a_4 + a_8 \left(\chi'' - \frac{\beta_\xi^+}{\beta^+} \right) - a_{10}\chi'' - a_{12}\frac{\beta_\eta^+}{\beta^+} \right) - \beta_\xi^- \right\} u_\xi^-$$

$$+ \left\{ a_5 + a_6 + a_8 \left(\frac{\beta_\eta^-}{\beta^+} - \frac{\beta_\eta^+}{\beta^+} \right) + a_{12}(1-\rho)\,\chi'' - \beta_\eta^- \right\} u_\eta^-$$

$$+ \left\{ a_7 + a_8\rho - \beta^- \right\} u_{\xi\xi}^- + \left\{ a_9 + a_{10} + a_8\,(\rho - 1) - \beta^- \right\} u_{\eta\eta}^-$$

$$+ \left\{ a_{11} + a_{12}\rho \right\} u_{\xi\eta}^- + (\hat{T}_{ij} - C_{ij}) + O(h),$$

where

$$\hat{T}_{ij} = a_2\,w + a_{12}\,\frac{v'}{\beta^+} + \left(a_6 - \frac{a_8\,\beta_\xi^+}{\beta^+} + a_{12}\chi'' \right) w'$$

(4.11)
$$+ a_{10}\,w'' + \frac{1}{\beta^+} \left(a_4 + a_8 \left(\chi'' - \frac{\beta_\xi^+}{\beta^+} \right) - a_{10}\chi'' - a_{12}\frac{\beta_\eta^+}{\beta^+} \right) v$$

$$+ a_8 \left\{ \frac{[f]}{\beta^+} - \frac{\kappa^+\,w}{\beta^+} - w'' \right\}.$$

We can ensure that $T_{ij} = O(h)$ by requiring that each coefficient of $u^-, u_\xi^-, u_\eta^-,$ $u_{\xi\xi}^-, u_{\xi\eta}^-,$ and $u_{\eta\eta}^-$ vanish, as well as the term $(\hat{T}_{ij} - C_{ij})$. This gives seven equations for the unknowns $\gamma_1, \ldots, \gamma_6$ and C_{ij}. The first six equations gives a linear system for the γ's (recall that each a_j is a linear combination of the γ's, given by (3.26), and that $\rho = \beta^-/\beta^+$):

$$a_1 + a_2 - a_8\,[\kappa]/\beta^+ = 0,$$

$$a_3 + \rho a_4 + a_8(\beta_\xi^- - \rho\beta_\xi^+ - [\beta]\chi'')/\beta^+$$

$$+ a_{10}[\beta]\chi''/\beta^+ + a_{12}(\beta_\eta^- - \rho\beta_\eta^+)/\beta^+ = \beta_\xi^-,$$

(4.12)
$$a_5 + a_6 - a_8[\beta_\eta]/\beta^+ + a_{12}(1-\rho)\,\chi'' = \beta_\eta^-,$$

$$a_7 + a_8\,\rho = \beta^-,$$

$$a_9 + a_{10} + a_8\,(\rho - 1) = \beta^-,$$

$$a_{11} + a_{12}\,\rho = 0.$$

Once the γ_j's are computed, we can easily obtain C_{ij} as

(4.13)
$$C_{ij} = \hat{T}_{ij},$$

where $\hat{T}_{ij}$ is given by (4.11).

The remarks at the end of the §3 still hold. Moreover, in the case where β and κ are continuous but vary with x and y, we see that the set of equations (4.12) reduces to

$$\begin{aligned} a_1 + a_2 &= 0, \\ a_3 + a_4 &= \beta_\xi, \\ a_5 + a_6 &= \beta_\eta, \\ a_7 + a_8 &= \beta, \\ a_9 + a_{10} &= \beta, \\ a_{11} + a_{12} &= 0. \end{aligned}$$

This set of equations is satisfied to $O(h^2)$ by using the five-point stencil with

$$\gamma_1 = \beta_{i-1/2,j}/h^2, \qquad \gamma_2 = -(\beta_{i-1/2,j} + \beta_{i+1/2,j} + \beta_{i,j-1/2} + \beta_{i,j+1/2})/h^2,$$

$$\gamma_3 = \beta_{i+1/2,j}/h^2, \qquad \gamma_4 = \beta_{i,j-1/2}/h^2, \qquad \gamma_5 = \beta_{i,j+1/2}/h^2, \qquad \gamma_6 = 0.$$

These are the coefficients for the standard formula (3.3).

5. Numerical results. We have done many numerical tests that confirm the expected order of accuracy for the immersed interface approach. We will present a few examples in two dimensions. In all of these examples Γ is the circle $x^2 + y^2 = \frac{1}{4}$ within the computational domain $-1 \le x, y \le 1$. See Fig. 1.

Example 1. In this example we compare our method with the discrete delta function approach for a problem where there is a singular source term along Γ. The differential equation is

(5.1) $$u_{xx} + u_{yy} = \int_\Gamma^2 \delta(x - X(s))\, \delta(y - Y(s))\, ds.$$

We use the Dirichlet boundary condition which is determined from the exact solution

(5.2) $$u(x,y) = \begin{cases} 1 & \text{if } r \le \frac{1}{2}, \\ 1 + \log(2r) & \text{if } r > \frac{1}{2}, \end{cases}$$

where $r = \sqrt{x^2 + y^2}$. From the equation we know that $[\partial u/\partial n] = 2$ at all points on Γ.

For the discrete delta function method we take m points on the interface Γ, where $m = n = 2/\Delta x = 2/\Delta y$ is the also number of uniform grid points in each direction. In the numerical experiments we have found that beyond this point, increasing the number of points on the interface gives little improvement in the solution. We use Peskin's discrete delta function (1.4). We have also tested the hat delta function defined in (1.3) and the numerical results are almost the same.

Figure 4 shows the results of both methods. We see that our method accurately gives the jump in the normal direction while the discrete delta function approach smears the jump, resulting in first-order accuracy.
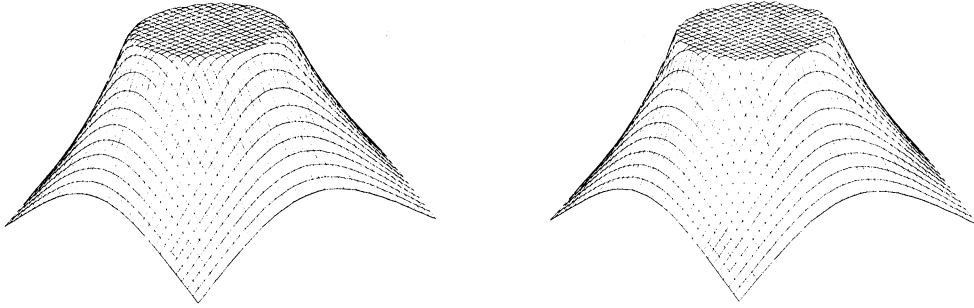
FIG. 4. *Comparison of two methods in Example 1.* (a) *The discrete delta function approach.* (b) *The immersed interface method.*

TABLE 1
Numerical results for Example 1.

n	Discrete delta function		Immersed interface method			
	$\| E_n \|_\infty$	Ratio	$\| E_n \|_\infty$	Ratio	$\| T_n \|_\infty$	Ratio
20	3.6140×10^{-1}		2.3908×10^{-3}		2.8276×10^{-1}	
40	2.6467×10^{-2}	12.7939	8.3461×10^{-4}	2.8646	1.6922×10^{-1}	1.6710
80	1.3204×10^{-2}	2.0045	2.4451×10^{-4}	3.4134	8.3449×10^{-2}	2.0278
160	6.6847×10^{-3}	1.9753	6.6856×10^{-5}	3.6573	4.1892×10^{-2}	1.9920
320	3.3393×10^{-3}	2.0018	1.5672×10^{-5}	4.2658	2.3049×10^{-2}	1.8175

Table 1 shows the results of a grid refinement study. The maximum error over all grid points,

$$\| E_n \|_\infty = \max_{i,j} | u(x_i, y_j) - u_{ij} |,$$

is presented, where u_{ij} is the computed approximation at the uniform grid points (x_i, y_j). For our method we also display $\| T_n \|_\infty$, the infinity norm of the local truncation error over all grid points. The local truncation errors are $O(h^2)$ except at those points that are close to the interface, where they are $O(h)$. We also display the ratios of successive errors,

$$\text{ratio} = \| E_{2n} \|_\infty / \| E_n \|_\infty \quad \text{or} \quad \| T_{2n} \|_\infty / \| T_n \|_\infty.$$

A ratio of 2 corresponds to first-order accuracy, while a ratio of 4 indicates second-order accuracy. We will use the same notation for other examples in this section.

Example 2. We now consider a problem with discontinuous coefficients as well as a singular source term. The equations are

(5.3) $$(\beta u_x)_x + (\beta u_y)_y = f(x,y) + C \int_\Gamma \delta(\vec{x} - \vec{X}(s)) \, ds$$

with $$f(x,y) = 8(x^2 + y^2) + 4,$$

$$\beta(x,y) = \begin{cases} x^2 + y^2 + 1 & \text{if } x^2 + y^2 \le \frac{1}{4}, \\ b & \text{if } x^2 + y^2 > \frac{1}{4}. \end{cases}$$

Dirichlet boundary conditions are determined from the exact solution

$$(5.4) \qquad u(x,y) = \begin{cases} r^2 & \text{if } r \le \frac{1}{2}, \\ (1 - \frac{1}{8b} - \frac{1}{b})/4 + (\frac{r^4}{2} + r^2)/b + C \log(2r)/b & \text{if } r > \frac{1}{2}. \end{cases}$$

It is easy to check that (5.4) satisfies (5.3). Table 2 gives numerical results for the case $b = 10$, $C = 0.1$. Again the local truncation error near Γ is only $O(h)$, but the resulting global error is seen to be $O(h^2)$. Figure 5 shows the computed solution for the case $b = 10$, $C = 0.1$ and $b = -3$, $C = 0.1$, respectively. In the first case, $\beta^- \beta^+ > 0$. As we mentioned in §3 the resulting linear system is "almost" symmetric positive definite. We use the LSOR method with the optimal relaxation parameter for the Poisson equation on the square. In the second case $\beta^- \beta^+ < 0$. The computed solution has the same accuracy as in the first case. In this case we used the Gauss–Seidel iteration.

TABLE 2

Numerical results for Example 2 with $b = 10, C = 0.1$.

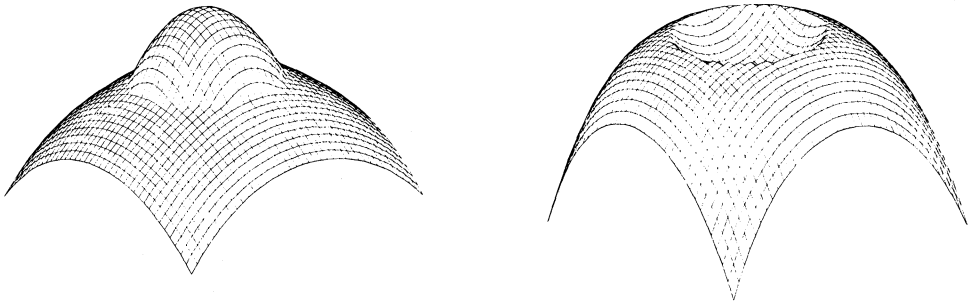| n	$\| E_n \|_\infty$	Ratio	$\| T_n \|_\infty$	Ratio
20	3.5195×10^{-3}		6.3843×10^{-1}	
40	7.5613×10^{-4}	4.6547	3.5988×10^{-1}	1.7740
80	1.6512×10^{-4}	4.5792	1.8999×10^{-1}	1.8942
160	3.6002×10^{-5}	4.5864	9.7499×10^{-2}	1.9487
320	8.4405×10^{-6}	4.2655	4.9374×10^{-2}	1.9747

FIG. 5. *The solutions for Example 2.* (a) *The function u for the case where $b = 10, C = 0.1$.*
(b) *The function $-u$ in the case where $b = -3, C = 0.1$.*

Example 3. In this example we impose a jump in the function u itself and also a jump in the normal derivative of u as external constraints. The differential equation

on each side of the interface is simply the Laplace equation

$$u_{xx} + u_{yy} = 0.$$

The jumps in u and $\partial u/\partial n$ are chosen so that the following function is the exact solution:

$$(5.5) \qquad u(x,y) = \begin{cases} e^x \cos y & \text{if } r \leq \frac{1}{2}, \\ \\ 0 & \text{if } r > \frac{1}{2}. \end{cases}$$

From this we can compute the functions v and w in (4.2) and (4.3). Since $\beta \equiv 1$, the standard five-point stencil is used at each grid point and (4.13) is used to determine the right-hand side C_{ij}. Any fast Poisson solver can then be used to solve the resulting system, with Dirichlet boundary conditions $u = 0$ on $\partial\Omega$.

Figure 6(a) shows the computed results on a 40×40 grid. The discontinuity in u is captured sharply. Table 3 shows that we again obtain second-order accuracy at all grid points, even in the neighborhood of the discontinuity.
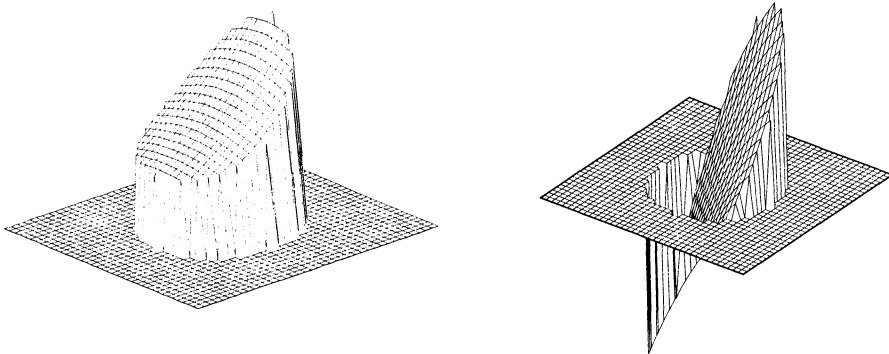

FIG. 6. *The solutions for Example 3, with jumps in u and its normal derivative specified along* Γ. (a) *For the solution* (5.5). (b) *For the solution* (5.6).

As a final test, we repeated this experiment with the exact solution

$$(5.6) \qquad u(x,y) = \begin{cases} x^2 - y^2 & \text{if } r \leq \frac{1}{2}, \\ \\ 0 & \text{if } r > \frac{1}{2} \end{cases}$$

shown in Fig. 6(b). In this case our method produced a computed solution with errors in the range $10^{-13} - 10^{-15}$ at all grid points (in double precision). This is expected since for the special case of a quadratic function the resulting truncation error should be identically zero, and only rounding errors appear in the computed solution (as amplified by the condition number of the matrix).

6. Summary. We have developed second-order accurate difference models for elliptic equations in the following situations: (i) The differential equations have discontinuous coefficients along a general interface. (ii) The differential equations have

TABLE 3
Numerical results for Example 3 with true solution (5.5).

n	$\| E_n \|_\infty$	Ratio	$\| T_n \|_\infty$	Ratio
20	4.37883×10^{-4}		2.99215×10^{-2}	
40	1.07887×10^{-4}	4.0587	1.52546×10^{-2}	1.9615
80	2.77752×10^{-5}	3.8843	7.70114×10^{-3}	1.9808
160	7.49907×10^{-6}	3.7038	3.87481×10^{-3}	1.9875
320	1.74001×10^{-6}	4.3098	1.93917×10^{-3}	1.9982

singular sources along a general interface. (iii) The differential equations have externally imposed constraints in the jump in u or normal derivatives of u across an interface. In all cases we are able to derive an appropriate difference stencil involving at most six grid points and the correct right-hand side so that the global error is $O(h^2)$ at all points on a uniform grid.

In the special case where the coefficients are continuous, the difference stencil reduces to the standard five-point stencil (3.3) and only the correct right-hand side must be derived to obtain second-order accuracy. In particular, if the coefficients are constant then the standard five-point Laplacian is used and a fast Poisson solvers can be used to solve the resulting linear system.

The ideas presented here can be used on a wide variety of other problems with discontinuous coefficients or singular sources. All that is required is that we be able to predict jumps in the solution and its first derivatives across Γ from the equation. These jumps are used in conjunction with appropriate Taylor series expansions about the interface to derive the difference scheme and right-hand side.

Other applications are currently being studied, including heat equations, wave equations in nonhomogeneous media, and the incompressible Navier–Stokes equations with flexible immersed boundaries.

REFERENCES

[1] R. E. ALCOUFFE, A. BRANDT, J. E. DENDY, AND J. W. PAINTER, *The multi-grid method for the diffusion equation with strongly discontinuous coefficients*, SIAM J. Sci. Statist. Comput., 2 (1981), pp. 430–454.

[2] K. AZIZ AND A. SETTARI, *Petroleum Reservoir Simulation*, Applied Science Publishers, New York, 1979.

[3] R. E. BANK, PLTMG: *A Software Package for Solving Elliptic Partial Differential Equations, User's Guide* 6.0, Society for Industrial and Applied Mathematics, Philadelphia, PA, 1990.

[4] J. B. BELL, P. COLELLA, AND H. M. GLAZ, *A second-order projection method for the incompressible navier-stokes equations*, J. Comput. Phys., 85 (1989), pp. 257–283.

[5] J. B. BELL, C. N. DAWSON, AND G. R. SHUBIN, *An unsplit, higher order Godunov method for scalar conservation laws in multiple dimensions*, J. Comput. Phys., 74 (1988), pp. 1–24.

[6] R. P. BEYER, *A computational model of the cochlea using the immersed boundary method*, J. Comput. Phys., 98 (1992), pp. 145–162.

[7] R. P. BEYER AND R. J. LEVEQUE, *Analysis of a one-dimensional model for the immersed boundary method*, SIAM J. Numer. Anal., 29 (1992), pp. 332–364.

[8] C. BÖRGERS AND O. WIDLUND, *On finite element domain imbedding methods*, SIAM J. Numer. Anal., 27 (1990), pp. 963–978.

[9] F. BRAKHAGEN AND T. W. FOGWELL, *Multigrid methods in modelling porous media flow*, in The Mathematics of Oil Recovery, Clarendon Press, New York, 1992, pp. 323–336.

[10] A. J. CHORIN, *Numerical solution of the Navier-Stokes equations*, Math. Comp., 22 (1968), pp. 745–762.

[11] J. CRANK, *Free and Moving Boundary Problems*, Oxford University Press, New York, 1984.

[12] L. FAUCI AND C. S. PESKIN, *A computational model of aquatic animal locomotion*, J. Comput. Phys., 77 (1988), pp. 85–108.

[13] L. J. FAUCI, *Interaction of oscillating filaments – a computational study*, J. Comput. Phys., 86 (1990), pp. 294–313.

[14] B. A. FINLAYSON, *Numerical Methods for Problems with Moving Fronts*, Ravenna Park Publishing, Seattle, WA, 1992.

[15] A. L. FOGELSON, *A mathematical model and numerical method for studying platelet adhesion and aggregation during blood clotting*, J. Comput. Phys., 56 (1984), pp. 111–134.

[16] A. L. FOGELSON AND C. S. PESKIN, *Numerical solution of the three dimensional stokes equations in the presence of suspended particles*, in Advances in Multiphase Flow and Related Problems, George Papaniculaou, ed., Society for Industrial and Applied Mathematics, Philadelphia, PA, 1986, pp. 67–74.

[17] B. FORNBERG AND R. MEYER-SPASCHE, *A finite difference procedure for a class of free boundary problems*, J. Comput. Phys., 102 (1992), pp. 72–77.

[18] R. J. MACKINNON AND G. F. CAREY, *Analysis of material interface discontinuities and superconvergent fluxes in finite difference theory*, J. Comput. Phys., 75 (1988), pp. 151–167.

[19] A. MAYO, *On the rapid evaluation of heat potentials on general regions*, IBM Tech. Report 14305.

[20] ———, *The fast solution of Poisson's and the biharmonic equations on irregular regions*, SIAM J. Numer. Anal., 21 (1984), pp. 285–299.

[21] ———, *Rapid, high order accurate evaluation of volume integrals of potential theory*, J. Comput. Phys., 100 (1992), p. 236.

[22] A. MAYO AND A. GREENBAUM, *Fast parallel iterative solution of Poisson's and the biharmonic equations on irregular regions*, SIAM J. Sci. Statist. Comput., 13 (1992), pp. 101–118.

[23] C. S. PESKIN, *Numerical analysis of blood flow in the heart*, J. Comput. Phys., 25 (1977), pp. 220–252.

[24] ———, *Lectures on mathematical aspects of physiology*, Lectures in Appl. Math., 19 (1981), pp. 69–107.

[25] G. R. SHUBIN AND J. B. BELL, *An analysis of the grid orientation effect in numerical simulation of miscible displacement*, Comput. Methods Appl. Mech. Engrg., 47 (1984), pp. 47–71.

[26] A. N. TIKHONOV AND A. A. SAMARSKII, *Homogeneous difference schemes*, USSR Comput. Math. and Math. Phys., 1 (1962), pp. 5–67.